PAPER

Check for updates

Nickel-containing 4,4′-biphenol mixed-mode stationary phase for the separation of polyaromatic compounds, benzene derivatives and nucleotides

Hira,[a] Faiz Ali, ID *[a] Muhammad Waqar,[a] Won Jo Cheong,[b] Munazzah[c] and Zeid A. AlOthman ID [d]

A new mixed-mode hybrid stationary phase is synthesized, followed by its characterization using BET analysis, SEM, FTIR spectroscopy and EDX analysis. 4, 4′-Biphenol was esterified using ethyl chloroacetate in the presence of potassium carbonate, followed by carboxylation using ethanol/water (9 : 1 v/v%) in the presence of NaOH. The product was treated with nickel nitrate hexahydrate, resulting in the formation of nickel-containing 4,4′-biphenol. The newly synthesized stationary phase was completely characterized through ^{1}H-NMR, ^{13}C-NMR, FTIR, EDX, FE-SEM, BET, particle size distribution, and XRD resulting in characteristics in line with proposed material and best fitting of the material to be used as the new separation media in liquid chromatography. The resultant material was packed in a stainless-steel column (200 mm long × 0.2 mm internal diameter) using a slurry packing machine and tested as a separation media in liquid chromatography. The newly developed column resulted in the separation of different analytes belonging to different classes, such as polyaromatic compounds (PACs), benzene derivatives, and a set of nucleotides, with average plate counts of 272 100, 243 000, and 244 800 plates m^{-1}, respectively, under the optimized mobile phase of acetonitrile/methanol/15 mM ammonium formate in the ratio of 60/30/10 v/v% at pH 6.5 and a flow rate of 25 μL min^{-1}.

Introduction

High performance liquid chromatography (HPLC) is one of the techniques usually used for analyzing and separating multi component mixtures.[1] HPLC separation modes are categorized according to the types of interactions between the analytes and stationary phases.[2] Single separation modes, such as reversed-phase liquid chromatography (RPLC), ion-exchange chromatography (IEC), and hydrophilic interaction liquid chromatography (HILIC), have been extensively reported, but such modes can only be used in limited applications. Multiple retention mechanisms in HPLC operating on a single column have recently been developed and encouraged for better separation with enhanced chromatographic performance.[3–6] Various types of mixed-mode chromatography (MMC), including RPLC/HILIC, RPLC/IEC, IEC/HILIC, and RPLC/IEC/HILIC, have been reported.[7–12]

Fast and efficient separation through HPLC depends on the selection of the materials used as the separation media, with the

stationary phase acting as the heart of HPLC.[13] A variety of stationary phases, such as chiral, chemically bonded cyclodextrin, molecularly imprinted polymer (MIP) monolith, and polysaccharide chiral stationary phases, have been documented for the enantioseparation of a wide range of analytes. Polymeric C18 and C8 stationary phases are used for the separation of PACs. Organic and polymeric monolith-, fluorocarbon-, and metal organic framework (MOF)-modified silica-based stationary phases have been used for analyzing biological samples such as nucleotide, proteins and peptides.[14–19]

Microporous materials consisting of metal ions linked through organic ligands known as MOFs are one of the recently developed materials serving as separation media in liquid chromatography due to their salient features, such as large surface area, higher throughput capacity, uniform structural cavities, better separation efficiency, and outstanding thermal and chemical stabilities.[20–23] Microporous organic networks (MONs) are another class of advanced microporous materials synthesized from aromatic alkynes and halide monomers via the Sonogashira–Hagihara coupling reaction.[24,25] The larger surface area and designable topology make them quite promising in various fields, such as catalysis,[26,27] contaminant removal,[28,29] sensing,[30] and gas storage processes.[31] Microporous organic polymers, including hyper crosslinked porous polymers[32] with intrinsic micro porosity and porous aromatic frameworks,[33] have attracted much attention in the recent past and at present.[34] The striking

[a] *Department of Chemistry, University of Malakand, Khyber Pakhtunkhwa, Pakistan. E-mail: faizy186@gmail.com; faiz@uom.edu.pk*

[b] *Department of Chemistry, Inha University, Incheon, South Korea*

[c] *Department of Medicine, Saidu Group of Teaching Hospitals, Swat, KPK, Pakistan*

[d] *Chemistry Department, College of Science, King Saud University, Riyadh 11451, Saudi Arabia*

features of MONs render them a good option for use in chromatographic separation and sample pretreatment.[35] The performance of any chromatographic method is determined by the physiochemical properties of the stationary phase.[36,37] It is important to explore new strategies for preparing new MON-based stationary phases exhibiting better interaction sites with multiple separation modes to improve the separation ability and selectivity of MONs in MMC.[38–41]

The current project aims to address and bridge this gap in the literature through the rational design, synthesis, and characterization of new MON-based stationary phases for mixed-mode HPLC applications. By developing multifunctional stationary phases, this study seeks to improve the selectivity, resolution, and efficiency of chromatographic separations for chemically diverse analytes to be analyzed and studied simultaneously. In addition to its technical contribution in terms of operational ease, it offers a strategic addition to the analytical science community, leading to better separation approaches for complex matrices in pharmaceutical, environmental, and biochemical studies. This study addresses potential limitations in material design and shows how MONs can improve separation performance in chromatography.

Materials and methods

Chemicals and reagents

4,4′-Biphenol (99%), potassium hydroxide (99.99%), sodium hydroxide (99%), nickel nitrate hexahydrate (99.99%) and potassium carbonate (99%) were purchased from Sigma-Aldrich (St. Loius, MO, USA). Ethyl chloroacetate (99%) and dimethyl formamide (DMF) (99.9%) were purchased from Heowns Biochemical Technology Co., Ltd. (Tianjin, China). HPLC-grade ethanol (99–100%) was obtained from Aladdin Biochemical Technology Co., Ltd. (Shanghai, China). Beaker, separating funnel, filter paper, spatula, dropper, Teflon vial, conical flask, digital balance (Shimadzu ATY 224), and pipette were used in the experimental work. A magnetic stirrer (Irmico, Germany) was used for stirring purposes. PAC, naphthalene (99%), fluorene (99%), anthracene (99%), triphenylene (98%), and benzene derivatives (such as phenol (99.9%), acetophenone (99%), nitro aniline (98.5%), 4-methyl-2-nitroaniline (98%), and xylene (99.5%)) were purchased from Sigma-Aldrich. The nucleotide adenosine monophosphate (AMP), uridine monophosphate (UMP), guanosine monophosphate (GMP), cytidine monophosphate (CMP), and uridine diphosphate (UDP) were obtained from Aladdin Biochemical Technology Co., Ltd.

Preparation of Ni-containing 4,4′-biphenol-based stationary phases

Synthesis of dimethyl 2,2′-[1,4-phenylenebis(oxy)]diacetate. 4,4′-Biphenol-based stationary phase was synthesized using the sophisticated renovated three-step procedure reported in the literature.[42,43] Dimethyl 2,2′-[1,4-phenylenebis(oxy)]diacetate (2) was synthesized in accordance with the procedure reported by our fellow research group.[44] Esterification of 4,4′-biphenol was carried out using 1.0 mmol of 4,4′-biphenol (1) dissolved in anhydrous DMF (10 mL), followed by the addition of potassium carbonate (2.0 mmol). Ethyl chloroacetate (2.2 mmol) was added dropwise under stirring conditions. The reaction mixture was treated at 80 °C for 12 h, cooled to room temperature and poured into ice-cold water. The resulting precipitate was filtered, washed with water, and dried at room temperature under a vacuum. The% yield of compound (2) is 81%.

Synthesis of the dicarboxylic acid ligand. Dimethyl 2,2′-[1,4-phenylenebis(oxy)]diacetate (2) (the esterified 4,4′-biphenol) was suspended in 20 mL of a solvent mixture containing 9 : 1 (v/v%) ethanol/water. Sodium hydroxide (2.5 mmol) was added to the reaction mixture and refluxed at 70 °C for 2 h, yielding the sodium salt of dicarboxylic acid (3) and ethyl alcohol as the side product. The sodium salt of dicarboxylic acid was subjected to protonation in an acidic environment to produce the dicarboxylic acid ligand. The solution was cooled and acidified with diluted HCl (at pH ∼ 2), and the resultant precipitated ligand 2,2′-([1,1′-biphenyl]-4,4′-diylbis(oxy)) diacetic acid (4) was collected by filtration, washed with water, and dried. The % yield of compound (4) is 78%.

Synthesis of 4,4′-biphenol-based microporous organic network. The carboxylated acid ligand (4) was dispersed in DMF (10 mL) under stirring conditions. 1.0 mmol of nickel(II) nitrate hexahydrate [Ni(NO$_3$)$_2$·6H$_2$O] was added to the solution and treated at 60 °C for 24 h. The resulting green precipitate was collected by filtration, washed with ethanol to remove the unreacted species, and dried at 120 °C under vacuum for 12 h, resulting in the formation of Ni containing 4,4′-biphenol-based microporous organic network (5). The entire synthesis scheme involving all the intermediates is illustrated in Fig. 1. The % yield of compound (5) is 76%.

The microscopic images of the particles of the final product showed a very large size. Therefore, the final product was manually ground using a mortar and pestle for 20 minutes or till the appearance of a fine powder-like nature. A microscope was used to take the images after grinding intervals of 5 min. After 20 minutes, there was no further effect of grinding on particle size, suggesting that the final size of the crustal was achieved. A slurry was prepared by dispersing 250 mg of the grounded phases in methanol.

Instrumentation

Setup of HPLC. Pressure pump, manual injector, solvent degasser, detector, and a homemade 200 mm glass-lined column with a 0.2 mm internal diameter were connected to construct an HPLC system. UV-2075 capillary window detector (Jasco, Japan), Shimadzu LC-10AD pump (Japan), C14W.05 injector with a 50 nL injection loop from Valco (Houston, TX, USA), and Shimadzu DGU-14A membrane degasser were connected. The final chromatographic results were evaluated using Origin Pro8 (Northampton, MA, USA). Lab solution (Shimadzu, Japan) software was installed to process the chromatographic data. The resultant chromatographic data were analyzed using Origin Pro 8.1.

Column packing. A stainless-steel column was packed by applying a pressure tapering strategy using a slurry packing
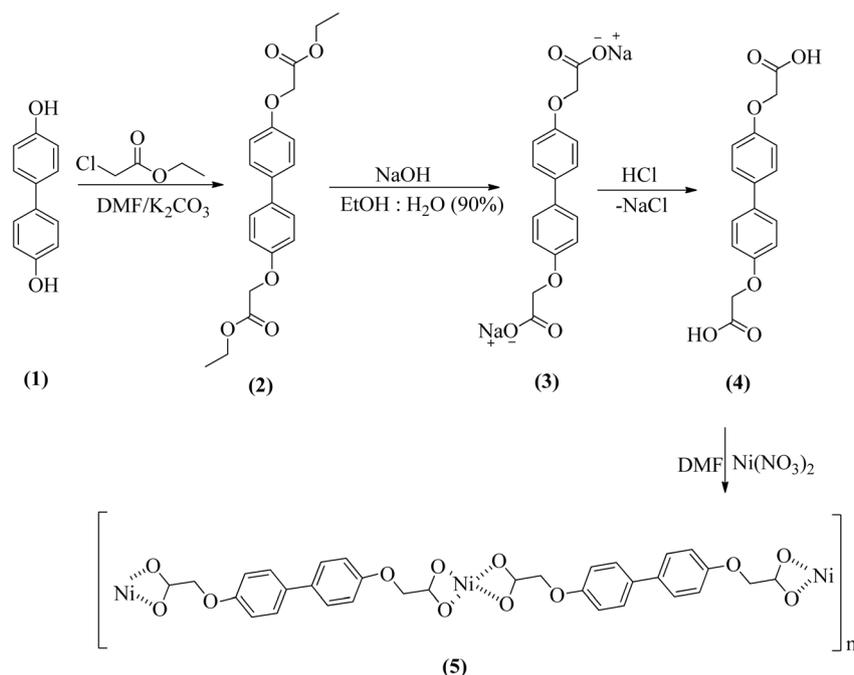
Fig. 1 Synthesis scheme for nickel-containing biphenol-based MONs through various intermediates.

machine. The reservoir of the slurry packing machine was fed with a stationary phase slurry. A home-assembled column with an outlet union with a 1 micrometer pore size screen frit was connected to the slurry packer (Altech, Deerfield, 1L, USA). The slurry was prepared by suspending nickel-containing the bisphenol-based stationary phase in methanol. The packing quality was improved by the simultaneous vibration of the reservoir and column during packing. The packer was operated using nitrogen gas at a pressure of 20 000 Psi for 5 min and then at 15 000 Psi for 15 min. Subsequently, the column was left in position until the pressure decreased to zero. The column was detached from the packer and connected to the HPLC injector on one side and to the UV detector on the other side. A set of nucleotides, PAC, and benzene derivatives was chosen to evaluate the separation performance of the newly developed column. The stock sample solution was stored below 4 °C. Theoretical plate numbers were calculated using the following equation:

$$N = 5.54[t_R/W_{(1/2)}]^2 \qquad (1)$$

where $W_{1/2}$ is the bandwidth at half height and t_R is the retention time.

Characterization

An Avance Bruker AM 300-MHz spectrophotometer with deuterated dimethyl sulfoxide (DMSO-d_6) was used for the structural confirmation of the synthesized ligands. Scanning electron microscopy (SEM), JSM 5910, JEOL Japan) was used to investigate the surface morphology, and Fourier-transform infrared FT-IR (PerkinElmer, spectrum version 10.5.1) was used to investigate the surface functionalities. A particle size

analyzer (Mastersizer 3000, USA), energy-dispersive X-ray (EDX) (JSM-6390LV), and Thermo Electron (Waltham, MA, USA) Flash EA1112 elemental analyzer were used to determine particle size distribution and elemental composition. Brunauer–Emmett–Teller and Barrett–Joyner–Halenda (BJH/BJH) nitrogen adsorption/desorption analysis were carried out using BEL-Japan (Osaka, Japan) BELSORP-MAX. An enduring pressure of less than 10^{-3} torr was obtained by degassing.
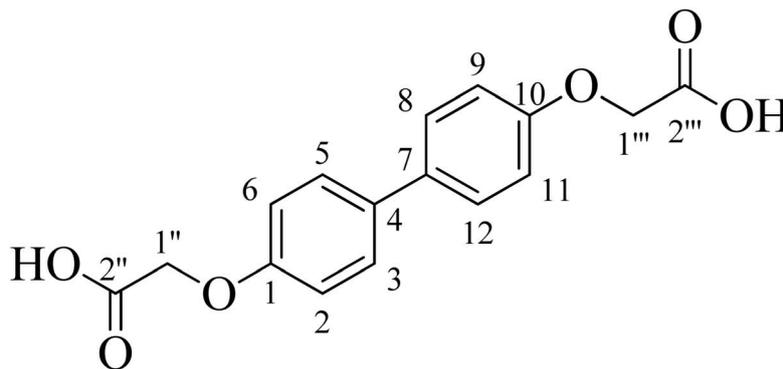
Results and discussion

^{1}H-NMR analysis

The ^{1}H-NMR spectrum (Fig. 2) of compound 2,2'-([1,1'-biphenyl]-4,4'-diylbis(oxy))diacetic acid (**4**) verifies the structure. The two aromatic doublets at δ 7.52 ppm ($J = 8.7$ Hz, 4H, ArCH-2,6,9,11) and δ 6.95 ppm ($J = 8.7$ Hz, 4H, ArCH-3,5,8,12) indicate a structure with symmetric *para*-disubstituted biphenyl. The singlet signal of four protons at δ 4.68 ppm corresponds to the two equivalent methylene groups (2CH$_2$-1″,1‴) linking the aromatic core to the diacetic acid moieties. The carboxylic acid (COOH) protons were not observed in the spectrum due to deuterium exchange in DMSO-d_6.
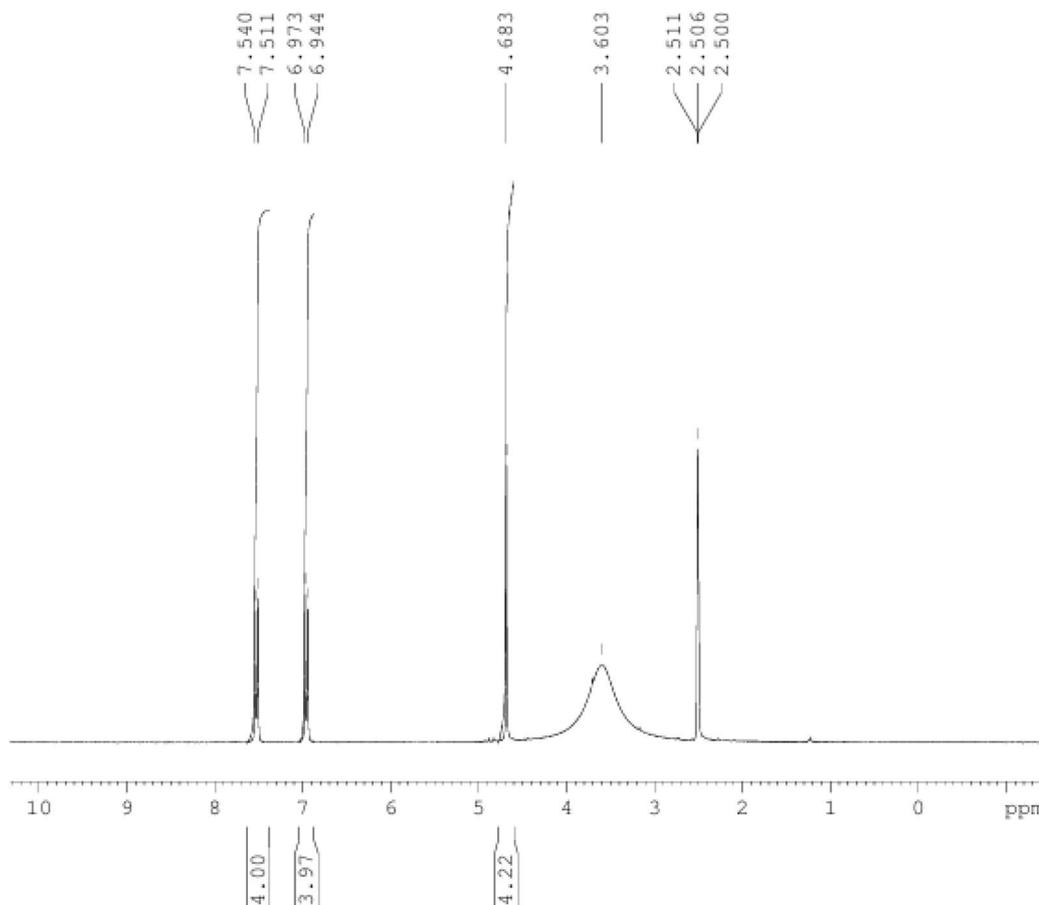
^{13}C-NMR analysis

The ^{13}C-NMR spectrum (Fig. 3) of 2,2'-([1,1'-biphenyl]-4,4'-diylbis(oxy))diacetic acid (**4**) in DMSO-d_6 further confirms the proposed structure. A resonance at δ 170.81 ppm can be attributed to the two equivalent carboxylic acid carbonyl carbons at position 2″,2‴. Signals at δ 157.40 ppm correspond to the two aromatic quaternary carbons bonded to the ether oxygen atoms (2ArC-1,10), while the resonance at δ 133.13 ppm

Fig. 2 ^{1}H NMR spectrum of 2,2′-([1,1′-biphenyl]-4,4′-diylbis(oxy))diacetic acid.

is due to the remaining quaternary aromatic carbons of the biphenyl core (2ArC-4,7). Aromatic methine carbons appear at δ 127.71 ppm (4ArCH-3,5,8,12) and δ 115.27 ppm (4ArCH-2,6,9,11), which are consistent with a symmetric *para*-disubstituted biphenyl system. A signal appearing at δ 65.07 ppm can be assigned to the two equivalent methylene carbons (2CH$_2$-1″,1‴) of the diacetic acid linker. The number and chemical shifts of the observed resonances are consistent with the molecular

structure, confirming the successful synthetic preparation of the target compound.

The intermediate compound labelled "product **2**" has already been reported by one of our fellow research groups, along with its complete spectral characterization. Instead of reproducing the same data, we cite the published work (ref. 44) for the ^{1}H NMR, ^{13}C NMR, and mass spectrometric data on compound (**2**). The final Ni-containing biphenol MOF product is a kind of coordination complex. Due to the paramagnetic
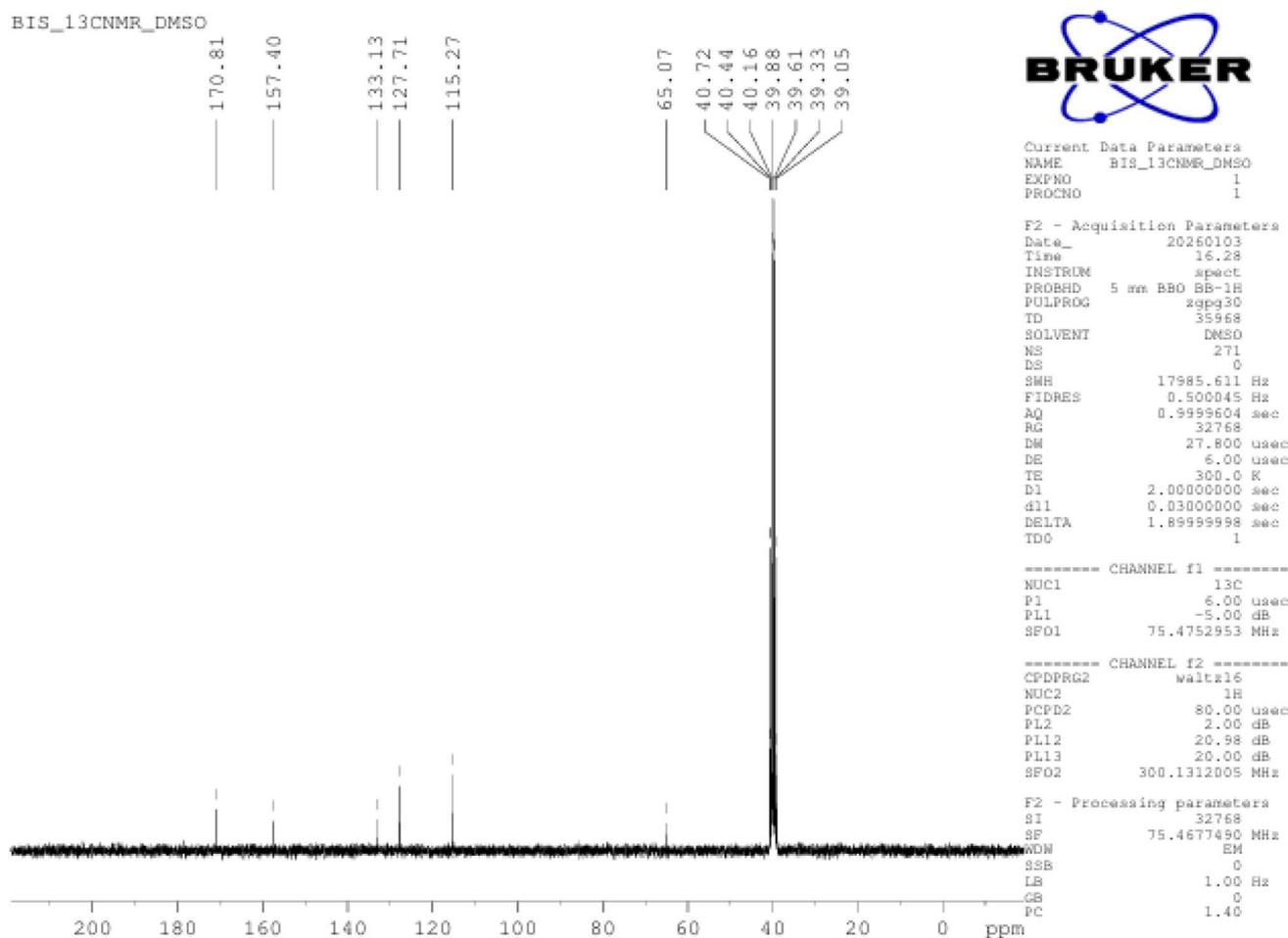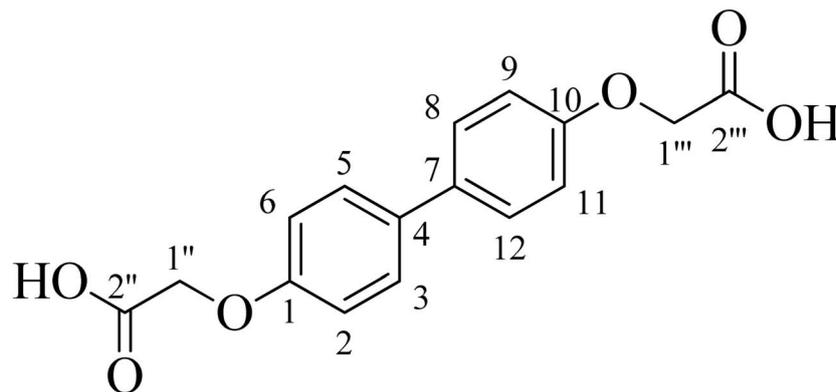
Fig. 3 ^{13}C NMR spectrum of 2,2'-([1,1'-biphenyl]-4,4'-diylbis(oxy))diacetic acid.

nature of the Ni(II) center, conventional ^{1}H and ^{13}C NMR spectroscopy are not suitable for the reliable structural analysis of this compound. Hence, NMR data on this complex could not be meaningfully obtained.

FT-IR analysis

The surface functionalities of the dicarboxylic acid ligand and the nickel-containing 4,4'-biphenol stationary phase were analyzed *via* FT-IR scanning in the range of 4000–500 cm^{-1} (Fig. 4). In the FT-IR spectrum of the dicarboxylic acid ligand (Fig. 4A), the broad peak appearing in the range of 2500–3300 cm^{-1} is the characteristic pattern for the O–H stretching vibrations of the carboxylic group. This broad peak is absent in the spectrum of the nickel-containing 4,4'-biphenol compound (Fig. 4B), indicating the involvement of the carboxyl-associated hydroxyl group in bonding with nickel ions, thereby confirming
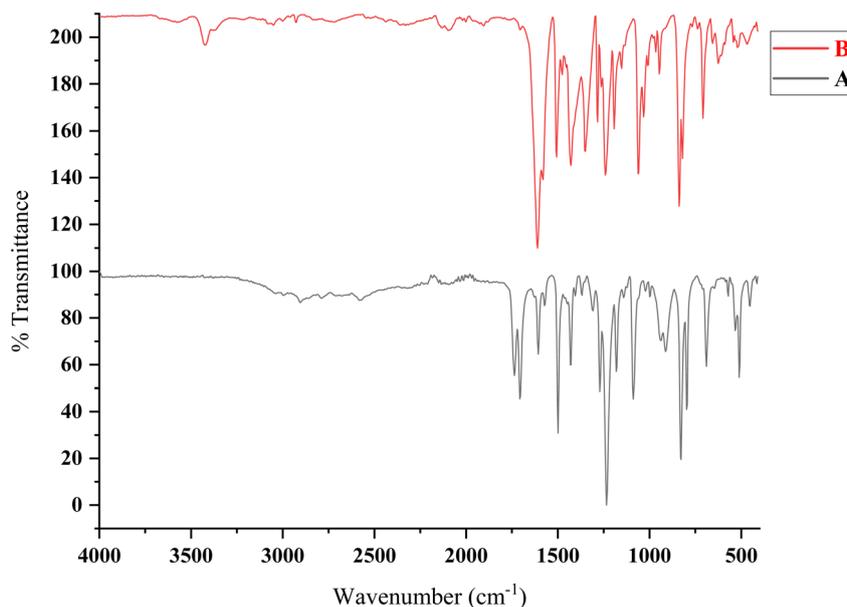
Fig. 4 FTIR spectra of dicarboxylic acid ligand (A) and nickel-containing 4,4′-biphenol-based stationary phase (B).

the formation of the nickel-containing 4,4′-biphenol compound. The band appearing at 3400 cm^{-1} in the spectrum (Fig. 4B) is attributed to the O–H stretching vibrations of hydroxyl groups originating from nickel nitrate hexahydrate.

Nickel coordination with the carboxylate group is further evidenced by the appearance of characteristic carboxylate stretching bands in the FT-IR spectrum of nickel-containing 4,4′-biphenol. A weak band at 1336 cm^{-1} corresponds to the symmetric stretching vibration of the carboxylate (–COO–) group, while a strong and intense band in the range of 1510–1650 cm^{-1} is assigned to the asymmetric stretching vibration of the carboxylate group. Further confirmation of product formation is obtained by comparing spectra A and B, where the characteristic carbonyl (C=O) stretching band of the carboxylic acid group observed at 1703 cm^{-1} in spectrum A disappears in spectrum B. This change arises from the deprotonation of carboxylic acid and the subsequent bonding with nickel ions.

Several absorption bands are common to both spectra. The band at 1606 cm^{-1} is attributed to the C=C stretching vibration of the aromatic rings present in 4,4′-biphenol. The peaks observed at 3037 and 3041 cm^{-1} correspond to aromatic C–H stretching vibrations, while the bands at 2907 and 2919 cm^{-1} are assigned to saturated C–H stretching vibrations. Overall, the FT-IR results provide strong evidence for the successful formation of the nickel-containing 4,4′-biphenol-based stationary phase.

Elemental analysis of the stationary phase

The EDX plots of the routine purified and extra purified 4,4′-biphenol-based stationary phase are illustrated in Fig. 5. The routine purified plot demonstrates C ∼ 44.07%, O ∼ 39.08%, and Ni ∼ 2.96%, while the extra-purified plot shows C ∼ 46.09%, O ∼ 37.04%, and Ni ∼ 4.95%. The presence of Cl and Na impurities suggests that the usual washing procedure is not

good enough to wash the products at steps 1 and 2 during the synthesis process, which comes from chloroethyl acetate and NaOH, respectively. Therefore, the final product was subjected to an additional and extra purification process by washing it thrice using a solvent mixture containing 2-propanol/water/ 0.1 M HCL (8 : 1:1 v/v%). The extra-purification washing strategy helped eliminate sodium and chloride ions. The EDX spectrum of the extra-purified material is depicted in Fig. 5B, where a diminished peak for sodium and chloride ions can be observed. Furthermore, the elemental composition using the Thermo Electron (Waltham, MA, USA) Flash EA1112 elemental analyzer confirmed the successful washing of the final product.

Thermo electron elemental analysis of the stationary phase

The carbon load of the nickel bound 4,4′-biphenol stationary phase particles of the current study (46.09%) is much higher than expected if it is compared to those of the previous studies reported in the literature.[14,15,19,20] The carbon load of the previously reported stationary phases is less than 20%, resulting in lower hydrophobic interaction.[14,15,19,20] A lower percentage of nickel in the stationary phase of the current study does not present a prominent effect on its chromatographic behavior but rather plays an effective role in the mixed-mode nature of the stationary phase. The percent composition of the resultant stationary phase consists of C ∼ 45.01%, H ∼ 13.07%, O ∼ 36%, and Ni ∼ 5%, which seems to have a well-balanced load of carbon, hydrogen, oxygen, and nickel.

Morphological appearance of nickel-containing 4,4′-biphenol

The morphology of nickel-containing 4,4′-biphenol particles is visualized in the form of SEM images before grinding (A) and after grinding (B) in Fig. 6. The SEM image before grinding suggests the crystalline nature of the particles, while after grinding, the
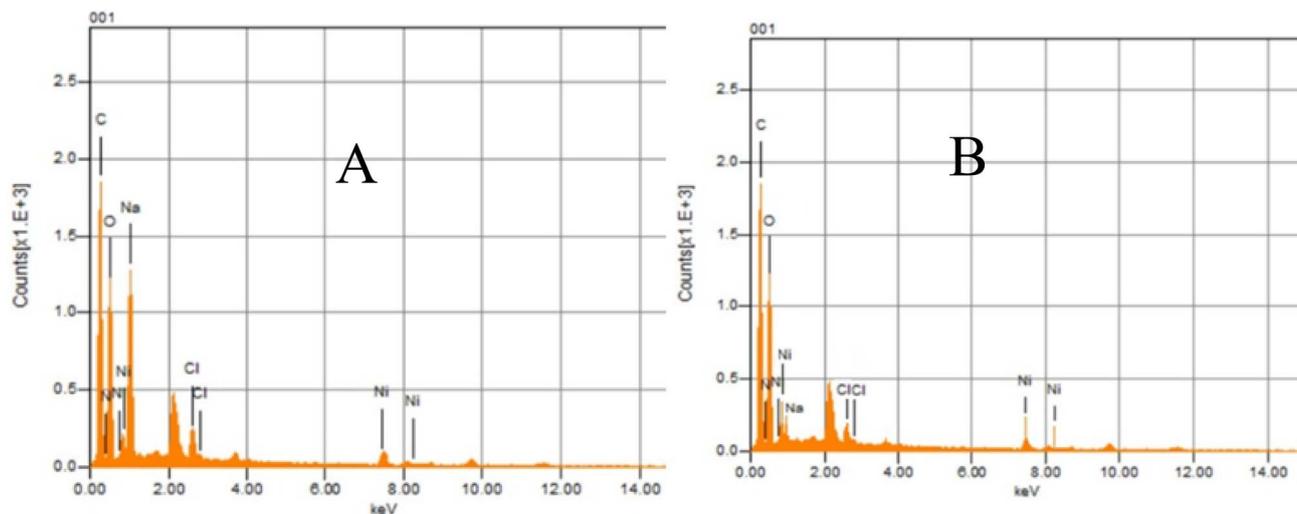
Fig. 5 EDX plots of nickel-bound 4,4′-biphenol: routine purified (A) and extra-purified (B).
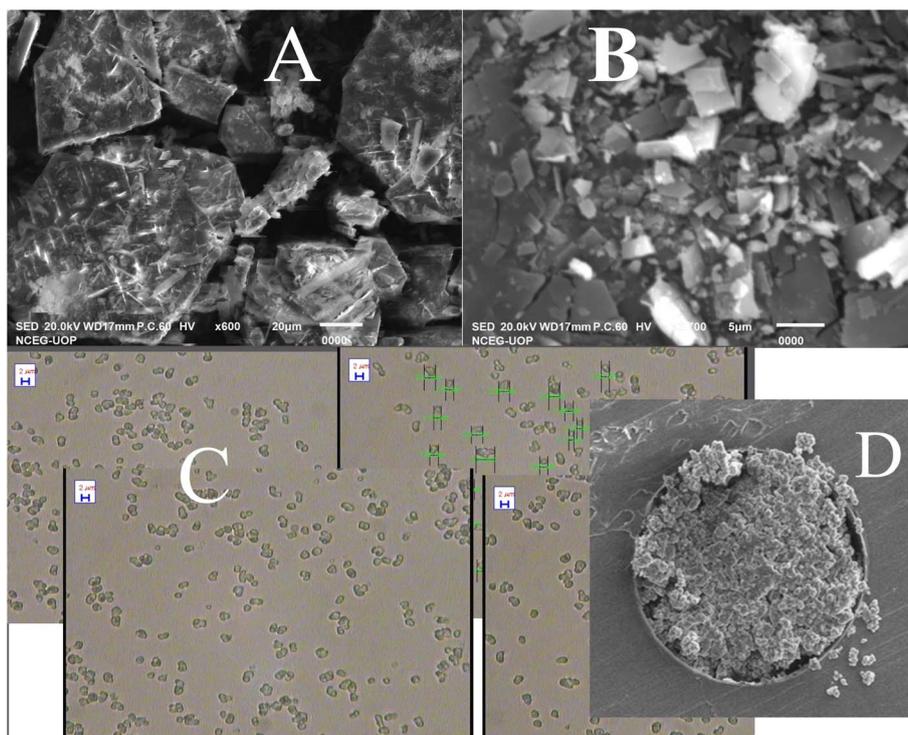

Fig. 6 SEM images before (A) and after (B) grinding, and microscopic images of nickel-containing 4,4′-biphenol particles (C). While (D) is the SEM image of the column section packed with the stationary phase after the chromatography application.

particles are reduced in particle size distribution down to sub 3 μm range with a good particle dispersity index shown in the microscopic images (Fig. 6C), and such characteristics render the resultant particles good enough for use as the stationary phase in liquid chromatography. Packing of the resultant stationary phase was quite challenging in a stainless-steel column, but the sophisticatedly renovated packing protocol was helpful in packing the particles. The SEM image of the column after chromatographic separation is depicted in Fig. 6D.

BET analysis

The pore size distribution data obtained from nitrogen adsorption and desorption isotherms suggest the porous nature of nickel-containing 4,4′-biphenol stationary phase. The BET pore size distribution plot of the resultant material is shown in Fig. 7A. The average pore size of the nickel-containing 4,4′-biphenol is 346 Å (34.6 nm) with an average pore volume of 0.899 cm^3 g^{-1}, suggesting the microporous nature of the newly synthesized material. Thus, the material synthesized in the
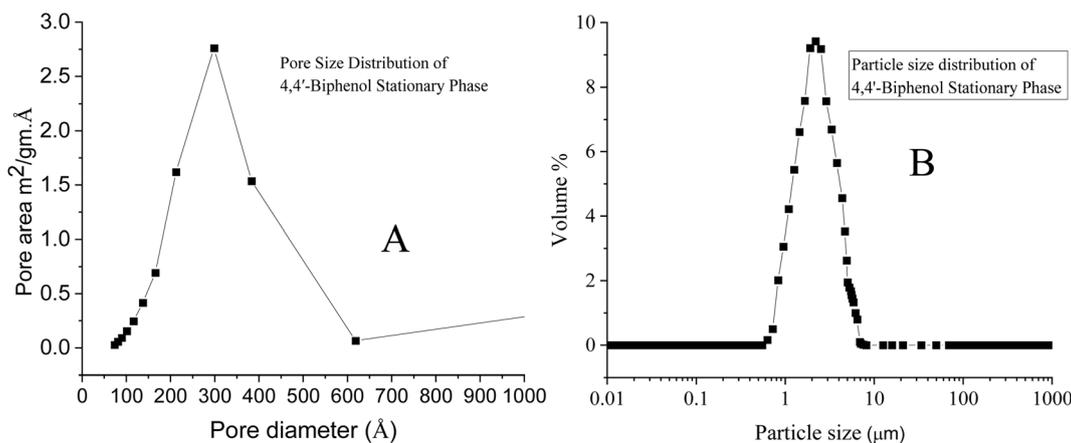
Fig. 7 BJH desorption (dA/dD) pore area (A) and particle size distribution (B) of the nickel-containing 4,4′-biphenol stationary phase.

current study can be regarded as microporous organic networks (MONs). The specific surface area of nickel-containing 4,4′-biphenol is 211 m^2 g^{-1}. Porous nature, pore size range (25–370 Å), pore volume (0.5–1 cm^3 g^{-1}), and surface area (100–400 m^2 G^{-1})[45–49] of the synthesized material agree with those of the previously reported values of the stationary phases or even the surface area is rather much better than those of the previous studies,[45] resulting in better chromatographic resolution of analytes belonging to different classes of compounds.

Particle size distribution

The volume % particle size of the final stationary phase is sub-3 μm as shown in Fig. 7B. Since particles of the resultant stationary phase are crystalline in nature, the crystal size, dimensions, and number of crystals present in the cluster determine the size of the particle, which in turn also depends on the synthesis procedure. The sizes of the finally obtained particles are well suited for use as the packing material in LC columns, demonstrating good chromatographic performance under HPLC conditions. The particle size distribution differentiated value at d (0.1) is 1.23, at d (0.5) is 2.42 μm, and at d (0.9) is 3.54 μm, suggesting the overall sub-3 μm particle size, as shown in the figure.

X-ray diffraction (XRD) of the stationary phase

The crystalline nature and structural integrity of the stationary phase were explored through XRD analysis. The XRD analysis suggests the crystalline nature of nickel-containing MOF stationary phase since all the peaks in the XRD spectrum illustrated in Fig. 8 are very narrow. Moreover, the peak pattern and distribution of peaks over the 2θ range are strongly in line with those of the reported spectrum of Ni containing MOF materials.[50–52] The spectrum shows peak diffractions at 2θ of 18.95°, 21.04°, 22.89°, 28.25°, 29.39°, 33.25°, 38.95°, and 42.4°.

Chromatographic evaluation of the stationary phase

The nickel-containing 4,4′-biphenol particles were evaluated as a new separation media after packing in a stainless-steel

column. The column developed in the current project was evaluated for the separation of a mixture of test analytes comprising PAC, benzene derivatives, and nucleotides. The set of selected PAC analytes contains benzene, naphthalene, fluorene, anthracene, and triphenylene. The set of selected benzene derivatives contains phenol, acetophenone, nitroaniline, 4-methyl-2-nitroaniline, and xylene, while the set of selected nucleotides contains AMP, CMP, GMP, UMP, and UDP. The elution conditions were optimized to achieve the best possible chromatographic performance of the column developed in the current study by applying different mobile phase compositions, where the optimized elution conditions were found to be acetonitrile/methanol 15 mM ammonium formate (60/30/10 v/v%) at pH 6.5, with a flow rate of 25 μL min^{-1} and a detection wavelength of 214 nm. The three sets of test analytes were separated under optimized elution conditions. The elution order of the test analytes was determined using the spiking procedure. The chromatograms illustrated in Fig. 9 demonstrated that good separation of the three sets of test analytes was
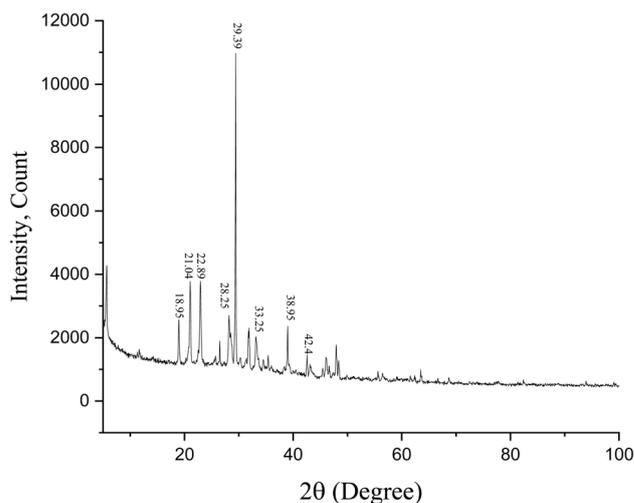

Fig. 8 XRD patterns from nickel-containing biphenol MOF stationary phase.
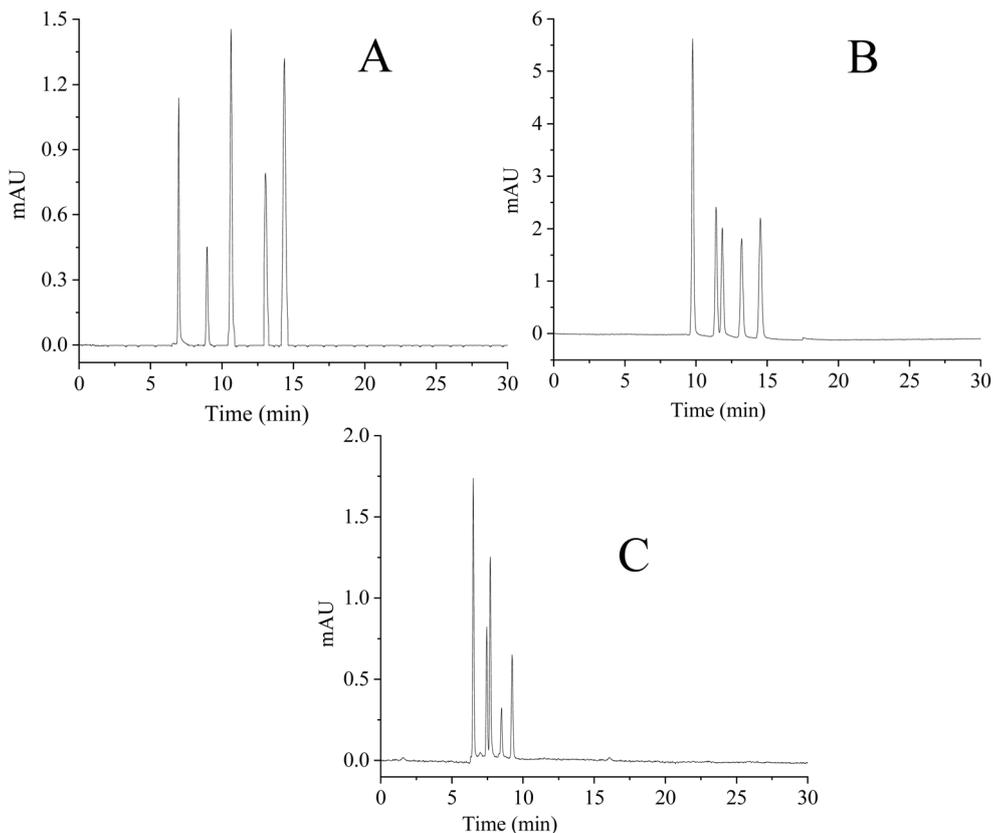
Fig. 9 Chromatograms of (A) PAC, (B) benzene derivatives, and (C) nucleotides using acetonitrile/methanol/15 mM ammonium formate (60/30/10 v/v%) at pH 6.5, flow rate of 25 μL min^{-1}, detection wavelength of 214 nm, column back pressure: 72 bar, column dimensions: 20 cm long $\times$ 0.2 mm ID.

obtained under the optimized elution conditions of the mobile phase with enhanced separation efficiency of 272 100 plates m^{-1}, 243 000 plates m^{-1}, and 244 800 plates m^{-1} for the PAC, benzene derivatives, and nucleotides, respectively. The plate count and resolution data obtained with the column in the current study are summarized in Tables 1 and 2, respectively. The resolution between the adjacent pairs of test analytes was checked for three runs taken on the same day and a single run taken for three consecutive days under the same elution conditions, where the average resolution values for the set of PAC, benzene derivatives, and nucleotides are 7.2, 3.6, and 2.7, respectively (Table 2). Since the resolution between two adjacent peaks is associated with chemistry of the stationary phase and the stationary phase is the same so selectivity will remain intact with no change in resolution. The earlier eluting peaks are sharper, as can be observed from the chromatogram, than the

latter eluting peaks under the isocratic elution mode. In addition to small particles and good packing protocol, the chemistry of the stationary phase is also very critical for improved separation since fine-tuned interaction of analytes with mobile and stationary phases is the key determinant parameter for obtaining high separation efficiency and resolution and hence the overall chromatographic performance.

Comparative study

The newly synthesized stationary phase and the resultant column of the current study were compared to those of the other stationary phases reported in the literature in view of the following points.

Separation efficiency. The efficient and rapid HPLC separation was obtained using core shell particles, monolith

Table 1 Separation efficiency of the column in the current study in terms of average N-value meter^{-1} for three sets of analytes

Analyte	N-Value	Analyte	N-Value	Analyte	N-value
Benzene	290 500	Phenol	252 500	AMP	219 500
Naphthalene	288 500	Acetophenone	252 000	CMP	219 500
Fluorene	269 000	Nitroaniline	248 500	GMP	213 000
Anthracene	262 000	4-Methyl 2-nitroaniline	236 000	UMP	321 500
Triphenylene	250 500	Xylene	226 000	UDP	250 500

Table 2 Resolution (R) between the adjacent pairs of analytes for PAC, benzene derivatives, and nucleotides computed using the column in the current study

Analyte	R	Analyte	R	Analyte	R
Benzene-naphthalene	8.3	Phenol-acetophenone	6.5	AMP-CMP	4.5
Naphthalene-fluorene	6.5	Acetophenone-nitroaniline	1.8	CMP-GMP	1.5
Fluorene-anthracene	9.1	Nitroaniline-4-methyl 2-nitroaniline	3.2	GMP-UMP	2.3
Anthracene-triphenylene	4.8	4-Methyl 2-nitroaniline-xylene	3.1	UMP-UDP	2.4
Average	7.2		3.6		2.7

stationary phases, tiny porous particles, and C-18 bound silica monolith particles.[46–48] A detailed comparative study of mass transfer kinetics for the stationary phases comprising tiny porous particles, monoliths, and core shell types has been reported. In the current study, a nickel-containing 4,4′-biphenol microporous organic network was synthesized and evaluated as the separation media under the optimized elution conditions of acetonitrile/methanol/15 mM ammonium formate (60/30/10 v/v%) with a flow rate of 25 μL min^{-1}, and the column backpressure was 72 bar. The irregular shape and nature of the particles, as shown in Fig. 6, are important for creating monolith-like architecture in the packed bed with flow through channels,[49] while the well-spread stationary phase particles, as can be observed in the microscopic image (Fig. 6C), are critical for good quality packing in contrast to the agglomerated particles. The agglomerated nature of stationary phase particles is one of the main issues responsible for poor packing beds, leading to degraded mass transfer kinetics.[52] In the current study, there was no issue of particle aggregation, and improved packing was achieved quite easily. Enhanced separation efficiency of the stationary phase of the current study, as illustrated in Table 1, in terms of theoretical plates corresponding to the chromatogram depicted in Fig. 9, was achieved due to the fine-tuned chemistry responsible for better interaction with selected sets of analytes and good quality packings.[52] Sub-3 μm particle size, though slightly higher than those of the reported stationary phases, exhibited improved chromatographic performance, suggesting that particle size is not the only determinant of chromatographic outcome. The results of the current study revealed that, in addition to particle size, other parameters must also be kept in the loop while striving for enhanced separation with an improved set of analytical figures of merit, such as separation efficiency, resolution, capacity factor, selectivity, and permeability. The average number of theoretical plates meter^{-1} obtained on the newly developed column of the current study is 272 100 m^{-1} for PAC, 243 000 m^{-1} for benzene derivatives, and 244 800 m^{-1} for nucleotides. The plate count for nucleotides obtained with the newly developed column is far better than that of ref. 53. The numerical values for the separation efficiencies of nucleotides are not presented in ref. 53, but the N-value meter^{-1} for various nucleotides can easily be estimated from the peak width in chromatograms. Similarly, the average N-value meter^{-1} obtained using the column of the current study for small molecules, like benzene derivatives, is higher (243 000 m^{-1}) than that (226 100 m^{-1}) of the previous study.[49]

Resolution. The average resolution between the four adjacent pairs was computed and compared with that of commercially available columns.[54] The minimum resolution between each set of two adjacent pairs for each of the three classes of analytes is computed, and their numerical values are illustrated in Table 2. The average resolution obtained for PAC analytes, benzene derivatives, and nucleotides is 7.2, 3.6, and 2.7, respectively (Table 2). The average resolution of all the three sets of test analytes is comparable with those of previous studies reported for other stationary phases under closely related elution conditions. Similarly, the average resolution among the adjacent pairs of analytes is comparable to that of the commercially available stationary phases.[54] The reproducibility in resolution was found to be excellent with %RSD values less than 0.5% for the day-to-day and column-to-column evaluations of the current study, which is because the chemistry of the stationary phase remains the same.

The optimum value for h (reduced particle size) as small as 1.2 can be observed for a good system composed of a column packed with ideal core shell particles.[55] The maximum value of N is 48 000 per column if a column of 4.6 mm internal diameter and 15 cm length packed with 2.6 μm core–shell particles is considered. A maximum N value per column of 37 500 was obtained for 1-chloro-4-nitrobenzene packed with 2.2 μm Halo core shell particles.[56] The maximum length of a commercial column packed with sub-3 μm particles is 15 cm. Besides, smaller particle size and good packing quality chemistry of the stationary phase are also very critical for obtaining good chromatographic parameters since fine-tuned interaction of analytes with mobile and stationary phases is the key determinant for obtaining high separation efficiency and resolution and hence the overall chromatographic performance. The column dimensions of the current study are 0.2 mm internal diameter and 20 cm length. The achievement of enhanced chromatographic variables with the column of the current study despite the relatively larger particle size might be due to the favorable chemistry and interactions of analytes with the stationary phase. Thus, the relatively larger particle-based stationary phase with fine-tuned chemistry results in higher permeability, on one hand, and improved separation efficiency and resolution, on the other hand, by critically altering the capacity factor of the stationary phase.

Reproducibility. To explore the application potentials of the column packed with nickel containing microporous organic network stationary phase in real samples, the reproducible nature of the column in terms of separation efficiency, retention

time, and column back pressure is very important with permissible %RSD values from an analytical chemistry viewpoint. The reproducibility of the column of the current study was evaluated following the standard procedure for all the three sets of test analytes under study. Three batches of the same stationary phase were synthesized and packed in three columns of similar dimensions using the same protocol for batch-to-batch reproducibility, while for inter-day reproducibility, one of the three columns was evaluated on three days. For column-to-column reproducibility, three columns were packed with a single batch of the resultant material and checked on the same day. The average %RSD in plate count for the column-to-column study is less than 5%, for inter-day is less than 2%, and

for batch-to-batch is less than 6.5%, while the average %RSD in retention time for column-to-column is less than 3% (Table 3), which is within the permissible limit of analytical chemistry. Column-to-column reproducibility in terms of column back pressure was checked using three columns of the same dimensions packed with a single batch of the stationary phase being synthesized in the current study, where the %RSD is 1.9%. Similarly, %RSD values for the inter-day, intraday, and batch-to-batch reproducibility on the column back pressure are 0.8%, 0.2%, and 2.1%, respectively (Table 4).

Permeability of the column. The lower column back pressure achieved in the current study is also one of the advantageous features of the current project, which might be due to the

Table 3 Column-to-column, inter-day, and batch-to-batch reproducibility of the column in terms of %RSD on plate counts and retention time for three batches of stationary phase synthesized using the same protocol[a]

| | Column-to-column | | | | Day-to-day | | Batch-to-batch | |
| | N-Value/meter | | Retention time (min) | | N-Value/meter | | N-value/meter | |
Analytes	Avg	%RSD	Avg	%RSD	Avg	%RSD	Avg	%RSD
Phenol	252 500	4.1%	10.11	2.6%	252 400	1.8%	252 600	5.3%
Acetophenone	252 000	3.2%	11.71	1.9%	252 100	1.7%	252 200	5.7%
Nitroaniline	248 500	3.9%	12.01	2.1%	248 300	1.6%	248 400	4.5%
4-Methyl-2-nitroaniline	236 000	4.8%	13.41	2.2%	236 100	2.1%	236 200	6.5%
Xylene	226 000	4.9%	14.80	2.8%	226 200	1.8%	226 100	5.1%
PAC								
Benzene	290 500	4.2%	6.71	2.5%	290 400	2.1%	290 600	5.2%
Naphthalene	288 500	3.9%	8.83	2.1%	288 300	1.8%	288 400	5.3%
Flourene	269 000	3.7%	11.01	2.3%	269 100	1.5%	269 200	4.9%
Anthracene	262 000	4.3%	13.05	2.4%	262 200	1.6%	262 300	5.1%
Triphenylene	250 500	4.5%	14.72	2.7%	250 400	2.2%	250 600	6.1%
Nucleotides								
AMP	219 500	4.2%	6.81	1.8%	219 400	1.6%	219 600	6.3%
CMP	219 500	3.8%	7.40	2.0%	219 300	1.7%	219 200	6.2%
GMP	213 000	3.9%	7.52	2.1%	213 100	1.8%	213 200	5.9%
UMP	321 500	4.4%	8.61	1.9%	321 600	2.0%	321 400	5.8%
UDP	250 500	4.7%	9.53	2.7%	250 400	1.9%	250 600	6.4%

[a] For column-to-column reproducibility data, three columns of the same dimensions were packed with the stationary phase of the current study, and the average N-values and retention times were calculated, while for day-to-day reproducibility, only the column packed with the stationary phase of the current study was evaluated on 3 consecutive days. Similarly, for assessing the batch-to-batch reproducibility, different batches of the stationary phase of the current study were synthesized by the same protocol, packed in a column of the same dimensions and evaluated for the separation of benzene derivatives, PACs, and nucleotides.

Table 4 Average column back pressure data for inter-day, intra-day, column-to-column, and batch-to-batch in terms of %RSD[a]

| | Intra-day | | Inter-day | | Column to column | | Batch to batch | |
	Avg	%RSD	Avg	%RSD	Avg	%RSD	Avg	%RSD
Column back pressure (bar)	71	0.2%	73	0.8%	72	1.9%	73	2.1%

[a] For the inter-day and intra-day data, the average was computed for a column packed with the stationary phase of the current study evaluated at three times within one day and on 3 consecutive days. For column-column pressure data, three columns of the same dimensions were packed with the stationary phase of the current study, and the average back pressure of the three columns was calculated. Similarly, for the batch-to-batch pressure data, different batches of the stationary phase of the current study were synthesized by the same protocol, packed in a column of the same dimensions and evaluated.

relatively larger particle size in comparison to those of the previous studies since the larger particle size offers low column back pressure at the expense of diminished plate counts. The permeability of the stationary phase of the newly developed column was computed using the following equation:

$$K = \frac{\mu\eta L}{\Delta P}, \qquad (2)$$

where η, Δp, L, and μ are the viscosity of the mobile phase, the backpressure of the column, the length of the column, and the mobile phase linear velocity, respectively. The permeability of the column (1.003×10^{-14} m^2) was computed using an acetonitrile/methanol 15 mM ammonium formate (60/30/10 v/v%). The permeability of the column in the current study is comparable to those of the monolith stationary phases reported in the literature.[52]

The %RSD in column back pressure was calculated to assess the column stability, and the numerical values are given in Table 4, suggesting that the column stability is good enough for the intra-day, inter-day, column-to-column and batch-to-batch analyses. The column back pressure under the optimized elution conditions is 72 bar.

Conclusion

A nickel containing 4,4′-biphenol-based stationary phase was synthesized. 4,4′-biphenol was reacted with ethyl chloroacetate to form dimethyl 2,2′-[1,4-phenylenebis(oxy)]diacetate, which was further treated with sodium hydroxide in a solvent mixture of ethanol and water (9:1), resulting in the formation of 2,2′-([1,1′-biphenyl]-4,4′-diylbis(oxy)) diacetic acid. Finally, the dicarboxylic acid ligand was treated with Ni(II) nitrate in DMF, resulting in the formation of a nickel-containing 4,4′-biphenol metal organic framework. The resultant material was extensively characterized through ^{1}H-NMR, ^{13}C-NMR, FTIR, EDX, FE-SEM, BET, particle size distribution, and XRD, with promising results and packed in a stainless column using an Alltech slurry packer. The newly developed column resulted in the separation of PACs, benzene derivatives, and nucleotides with improved chromatographic performance in terms of separation efficiency and resolution in HPLC. A higher number of theoretical plates (PACs = 272 100 m^{-1}, benzene derivatives = 243 000 m^{-1} and nucleotides = 244 800 m^{-1}) was obtained using the optimized mobile phase containing acetonitrile/methanol/15 mM ammonium formate (60/30/10 v/v%) at pH 6.5 and a flow rate of 25 μL min^{-1}.

Author contributions

Hira = data curation, formal analysis, and writing – original draft. Faiz Ali = conceptualization, methodology, project administration, resources, supervision, and validation. Muhammad Waqar = software supervision, review and editing. Won Jo Cheong = resources and review. Munazzah = formal analysis and investigation. Zeid A. AlOthman = investigation and resources.

Conflicts of interest

There are no conflicts to declare.

Data availability

The data supporting the findings of this paper are available as the supplementary information (SI). Even if needed further the corresponding author will provide material on request. Supplementary information is available. See DOI: https://doi.org/10.1039/d5ra08544f.

Acknowledgements

References

1 T. Salesch, S. Bachmann, S. Brugger, R. Schaefer, A. Mehdi and J. P. Corriu, New Inorganic±Organic Hybrid Materials for HPLC Separation Obtained by Direct Synthesis in the Presence of a Surfactant, *Adv. Funct. Mater.*, 2002, **12**(2), 134–142.

2 L. Wang, W. Wei, Z. Xia, X. Jie and Z. Z. Xia, Recent advances in materials for stationary phases of mixed mode high-performance liquid chromtography, *TrAC, Trends Anal. Chem.*, 2016, **80**, 495–50.

3 T. Walter, *et al.*, Characterization of a highly stable mixed-mode reversed-phase/weak anion-exchange stationary phase based on hybrid organic/inorganic particles, *J. Sep. Sci.*, 2021, **44**(5), 1005–1014.

4 S. Zhang, F. Zhang, B. Yang and X. Liang, A reversed phase/hydrophilic interaction/ion exchange mixed-mode stationary phase for liquid chromatography, *Chin. Chem. Lett.*, 2019, **30**(2), 470–472.

5 S. Zhang, Q. Wan and Y. Li, Epoxide-derived mixed-mode chromatographic stationary phases for separation of active substances in fixed-dose combination drugs, *J. Sep. Sci.*, 2019, **42**(17), 2796–2804.

6 D. Zhou, *et al.*, Preparation and evaluation of a reversed-phase/hydrophilic interaction/ion-exchange mixed-mode chromatographic stationary phase functionalized with dopamine-based dendrimers, *J. Chromatogr. A*, 2018, **1571**, 165–175.

7 C. Yuang, W. Jia and M. Zi, Are highly stable covelent organic frameworks the key to universal chiral stationary phases for liquid and gas chromatographic separations?, *J. Am. Chem. Soc.*, 2022, **144**(2), 891–900.

8 S. Hossieni and H. Tabar, Prepartion of two ammide-bonded stationary phases and comperative evalution under mixed-mode chromatography, *J. Sep. Sci.*, 2021, **44**(15), 2888–2897.

9 M. Liu, B. Li and Y. Zhou, Core shell metal organic framwork as the mixed mode stationary phase foe hydrophilic

interaction/reversed phase chromatography, *ACS Appl. Mater. Interfaces*, 2019, **11**(10), 10320–10327.

10 Q. Bai and X. Wang, Protien separation using a novel silica based RPLC/IEC mixed mode stationary phase modified with N-methylimidazolium ionic liquid, *Talanta*, 2018, **185**, 89–97.

11 Z. Chu and M. Zhu, Layer-by-layer coating and chemical cross-linked of multilayer polysaccharides on silica for mixed-mode HPLC application, *Chem. Commun.*, 2021, **57**(96), 12956–12959.

12 J. Fekete and K. Ganzler, Characterization of new types of stationary phases for fast liquid chromatographic applications, *J. Pharm. Biomed. Anal.*, 2009, **50**, 703–709.

13 H. Li, J. Quan and J. Chen, imidazolium ionic liquid-enhanced polu (quinine) modified silica s a new multi-mode chromatographic stationary phase for separation of achiral and chiral compounds, *Talanta*, 2020, **211**, 120743.

14 C. Lane and A. Stephen, Synthesis and characterization of polymeric C18 stationary phases for liquid chromatography, *Anal. Chem.*, 1984, **56**, 504–510.

15 J. Fekete and K. Ganzler, Characterization of new types of stationary phases for fast liquid chromatographic applications, *J. Pharm. Biomed. Anal.*, 2009, **50**, 703–709.

16 K. Zhang and X. Liu, Reprint of Mixed-mode chromatography in pharmaceutical and biopharmaceutical applications, *J. Pharm. Biomed. Anal.*, 2016, **130**, 19–34.

17 P. Jandera, Advances in the development of organic polymer monolithic columns and their applications in food analysis-A review, *J. Chromatogr. A*, 2013, **1313**, 37–53.

18 W. Zhang, Fluorocarbon stationary phases for liquid chromatography applications, *J. Fluorine Chem.*, 2008, **129**, 910–919.

19 J. Gao, Q. Wang and D. Xu, Recent advances in preparation and applications of monolithic chiral stationary phases, *TrAC, Trends Anal. Chem.*, 2020, **123**, 115774.

20 Z. Y. Gu, C. X. Yang, N. Chang and X. P. Yan, Metal–organic frameworks for analytical chemistry: from sample collection to chromatographic separation, *Acc. Chem. Res.*, 2012, **45**, 734–745.

21 Y. B. Yu, Y. Q. Ren, W. Shen, H. M. Deng and Z. Q. Gao, Applications of metal–organic frameworks as stationary phases in chromatography, *TrAC, Trends Anal. Chem.*, 2013, **50**, 33–41.

22 J. L. C. Rowsell and O. M. Yaghi, Metal–organic frameworks: a new class of porous materials, *Microporous Mesoporous Mater.*, 2004, **73**, 3–14.

23 M. Abdighahroudi, H. Lutze and T. Schmidt, Development of an LC-MS method for determination of nitrogen-containing heterocycles using mixed-mode liquid chromatography, *Anal. Bioanal. Chem.*, 2020, **412**(20), 4921–4930.

24 Y.-Y. Cui, X.-Q. He, C.-X. Yang and X.-P. Yan, Application of microporous organic networks in separation science, *TrAC, Trends Anal. Chem.*, 2021, **139**, 116268.

25 H.-F. Sun, Y.-Y. Cui, C.-Q. Zhen and C.-X. Yang, Monomer-mediated fabrication of microporous organic network@ silica microsphere for reversed-phase/hydrophilic

interaction mixed-mode chromatography, *Talanta*, 2023, **251**, 123763.

26 H. Lei, Y. Hu and G. Li, Magnetic poly (phenylene ethynylene) conjugated microporous polymer microspheres for bactericides enrichment and analysis by ultra-high performance liquid chromatography-tandem mass spectrometry, *J. Chromatogr. A*, 2018, **1580**, 22–29.

27 S.-W. Gao, N. Li, Y.-Y. Cui and C.-X. Yang, Modification of hollow microporous organic network with polyethyleneimine for efficient enrichment of phenolic acids from fruit juice samples, *J. Chromatogr. A*, 2024, **1736**, 465419.

28 Z.-D. Du, Y.-Y. Cui, C.-X. Yang and X.-P. Yan, Synthesis of magnetic amino-functionalized microporous organic network composites for magnetic solid phase extraction of endocrine disrupting chemicals from water, beverage bottle and juice samples, *Talanta*, 2020, **206**, 120179.

29 Q. Jiang, X. Xin, S. Zhang, S.-S. Wang, J. Feng and M. Sun, Advances of covalent organic frameworks as the stationary phases for liquid chromatography, *TrAC, Trends Anal. Chem.*, 2024, **174**, 117680.

30 C.-Y. Li, J.-M. Liu, Z.-H. Wang, S.-W. Lv, N. Zhao and S. Wang, Integration of Fe3O4@ UiO-66-NH2@ MON core-shell structured adsorbents for specific preconcentration and sensitive determination of aflatoxins against complex sample matrix, *J. Hazard. Mater.*, 2020, **384**, 121348.

31 K. Zhang, S.-L. Cai, Y.-L. Yan, Z.-H. He, H.-M. Lin, X.-L. Huang and W.-G. Zhang, Construction of a hydrazone-linked chiral covalent organic framework–silica composite as the stationary phase for high performance liquid chromatography, *J. Chromatogr. A*, 2017, **1519**, 100–109.

32 L. T. B. Tan, Hypercrosslinked porous polymer materials: design, synthesis, and applications, *Chem. Soc. Rev.*, 2017, **46**(11), 3322–3356.

33 Y. Yuan, F. Sun, H. Ren, X. Jing, W. Wang, H. Ma and G. Zhu, Targeted synthesis of a porous aromatic framework with a high adsorption capacity for organic molecules, *J. Mater. Chem.*, 2011, **21**(35), 13498–13502.

34 J. Li, H. Li, Y. Zhao, S. Wang, X. Chen and R.-S. Zhao, A hollow microporous organic network as a fiber coating for solid-phase microextraction of short-chain chlorinated hydrocarbons, *Microchim. Acta*, 2018, **185**(9), 416.

35 X. Li and Y.-Y. C. C.-X. Yang, Covalent coupling fabrication of microporous organic network bonded capillary columns for gas chromatographic separation, *Talanta*, 2021, **224**, 121914.

36 V. Halan, S. Maity, R. Bhambure and A. Rathore, Multimodal chromatography for purification of biotherapeutics – a review, *Curr. Protein Pept. Sci.*, 2018, **20**(1), 4–13.

37 W. Qin, M. E. Silvestre, F. Kirschofer, G. brenner-weiss and M. Franzeb, Insights into chromatography separation using core-shell metal-organic framework: size exclusion and polarity effects, *J. Chromatogr. A*, 2015, **1411**, 77–83.

38 D. Sýkora, P. Řezanka, K. Záruba and V. Král, Recent advances in mixed-mode chromatographic stationary phases, *J. Sep. Sci.*, 2018, **42**(1), 89–129.

39 Q. Wan, X. Wang and L. Chen, Inverse mixed-mode chromatography for the evaluation of multivalency and cooperativity of host–guest complexation in porous materials, *Langmuir*, 2019, **35**(32), 10405–10411.

40 J. Lee, J. Choi and D. Kang, Thin and small N-doped carbon boxes obtained from microporous organic networks and their excellent energy staorage performance at high current densities in coin cell supercapacitors, *ACS Sustain. Chem. Eng.*, 2018, **6**(3), 3525–3532.

41 J. Jang, H. Ko and J. Kim, Triple-double-, and single-shelled hallow spheres of sulfonated microporous organic network as drug delivery materials, *Chem. Mater.*, 2018, **31**(2), 300–304.

42 M. Ibrahim, A. Latif, Ammara, A. Ali, A. I. Ribeiro, U. Farooq and M. Ali, Macrocyclic sulfone derivatives: Synthesis, characterization, in vitro biological evaluation and molecular docking, *Drug Dev. Res.*, 2021, **82**(4), 562–574.

43 S. Rachel, R. Hanton and J. Sumby, Synthesis of zinc (II) dicarboxylate ligand metal organic framework (MOF): a potential precursor to MOF-tethered N-heterocyclic carbene compounds, *Inorg. Chem.*, 2010, **49**, 1712–1719.

44 M. Ibrahim, S. A. Halim, A. Latif, M. Ahmad, S. Ali, S. Ullah and M. Ali, Synthesis, biochemical and computational evaluations of novel bis-acylhydrazones of 2, 2′-(1, 1′-biphenyl)-4, 4′-diylbis (oxy) di (acetohydrazide) as dual cholinesterase inhibitors, *Bioorg. Chem.*, 2024, **144**, 107144.

45 M. Skoczylas, S. Bocian and B. Buszewski, *J. Chromatogr. A*, 2020, **1609**, 460514.

46 G. Sun and Y. Lu, Polystyrene immobilized sol-gel ground silica monolith particles using one-pot reaction of enhanced separation efficiency, *J. Chromatogr. Sci.*, 2021, **59**, 949–955.

47 G. Guiochen and F. Gritti, Shell particles, trials, tribulations and triumphs, *J. Chromatogr. A*, 2011, **1218**, 1915–1938.

48 G. Guiochon, Monolithic columns in high-performance liquid chromatography, *J. Chromatogr. A*, 2007, **1168**, 101–168.

49 F. Ali and W. Cheong, A simple and cost-effective hybrid stationary phase for separation of peptides, protein and benzene derivatives through liquid chromatography, *RSC Adv.*, 2024, **14**, 34486.

50 M. Faizy, S. Molaei and M. Ghadermazi, Synthesis and characterization of Ni-MOF and CoFe$_2$O$_4$/Ni-MOF as reusable heterogeneous catalysts for the synthesis of 5-substituted 1*H*-tetrazole, *Sci. Rep.*, 2025, **15**, 40090.

51 F. Israr, D. Chun, Y. Kim and D. K. Kim, High yield synthesis of Ni-BTC metal–organic framework with ultrasonic irradiation: Role of polar aprotic DMF solvent, *Ultrason. Sonochem.*, 2016, **31**, 93–101.

52 F. Ali, W. J. Cheong, Z. A. ALOthman and A. M. ALMajid, Polystyrene bound stationary phase of excellent separation efficiency based on partially sub-2 μm silica monolith particles, *J. Chromatogr. A*, 2013, **1303**, 9–17.

53 E. Tomiya, Ailor "Determination of nucleotides and sugar nucleotides involved in protien gylocosylation by high performance anion exchange chromatography: sugar nucleotides contant in cultured insects cells and mamalian cells", *Anal. Biochem.*, 2001, **293**(1), 129–137.

54 S. M. Lee, S. A. Zaidi and W. J. Cheong, A new stationary phase prepared from ground silica monolith particles by reversible addition-fragmentation chain transfer polymerization, *Bull. Korean Chem. Soc.*, 2010, **31**(10), 2943–2948.

55 E. Olah, S. Fekete, J. Fekete and K. Ganzler, Comparative study of new shell-type, sub-2 μm fully porous and monolith stationary phases, focusing on mass-transfer resistance, *J. Chromatogr. A*, 2010, **1217**(23), 3642–3653.

56 J. J. DeStefano, S. A. Schuster, J. M. Lawhorn and J. J. Kirkland, Performance characteristics of new superficially porous particles, *J. Chromatogr. A*, 2012, **1258**, 76–82.